



Interactive versus additive relationships between regional cortical thinning and amyloid burden in predicting clinical decline in mild AD and MCI individuals



Federico d'Oleire Uquillas^a, Heidi I.L. Jacobs^{b,c}, Bernard Hanseeuw^{b,c,d}, Gad A. Marshall^{a,e}, Michael Properzi^a, Aaron P. Schultz^{a,c}, Molly R. LaPoint^a, Keith A. Johnson^{b,c,e}, Reisa A. Sperling^{a,c,e}, Patrizia Vannini^{b,c,e,*}

^a Department of Neurology, Massachusetts General Hospital, Harvard Medical School, Boston, MA, USA

^b Department of Radiology, Massachusetts General Hospital, Harvard Medical School, Boston, MA, USA

^c Athinoula A. Martinos Center for Biomedical Imaging, Massachusetts General Hospital, Harvard Medical School, Charlestown, MA, USA

^d Department of Neurology, Saint-Luc University Hospital, Institute of Neuroscience, Université Catholique de Louvain, Brussels, Belgium

^e Department of Neurology, Brigham and Women's Hospital, Harvard Medical School, Boston, MA, USA

ARTICLE INFO

Keywords:

Alzheimer's disease
Beta-amyloid
Clinical decline
Cortical thickness
Medial temporal lobe
Mild cognitive impairment

ABSTRACT

The biological mechanisms that link Beta-amyloid (A β) plaque deposition, neurodegeneration, and clinical decline in Alzheimer's disease (AD) dementia, have not been completely elucidated. Here we studied whether amyloid accumulation and neurodegeneration, independently or interactively, predict clinical decline over time in a group of memory impaired older individuals [diagnosed with either amnesic mild cognitive impairment (MCI), or mild AD dementia]. We found that baseline A β -associated cortical thinning across clusters encompassing lateral and medial temporal and parietal cortices was related to higher baseline Clinical Dementia Rating Sum-of-Boxes (CDR-SB). Baseline A β -associated cortical thinning also predicted CDR-SB over time. Notably, the association between CDR-SB change and cortical thickness values from the right lateral temporo-parietal cortex and right precuneus was driven by individuals with high A β burden. In contrast, the association between cortical thickness in the medial temporal lobe (MTL) and clinical decline was similar for individuals with high or low A β burden. Furthermore, amyloid pathology was a stronger predictor for clinical decline than MTL thickness. While this study validates previous findings relating AD biomarkers of neurodegeneration to clinical impairment, here we show that regions outside the MTL may be more vulnerable and specific to AD dementia. Additionally, excluding mild AD individuals revealed that these relationships remained, suggesting that lower cortical thickness values in specific regions, vulnerable to amyloid pathology, predict clinical decline already at the prodromal stage.

1. Introduction

Deposition of Beta-amyloid (A β) plaques begins years before the onset of clinical symptoms present across the Alzheimer's disease (AD) dementia continuum (Selkoe and Hardy, 2016; Sperling et al., 2011) and continues to slowly accumulate (Jack et al., 2013; Villemagne et al., 2013; Walsh and Teplow, 2012). While A β deposition is only moderately associated with cognitive decline (Villemagne et al., 2011), neurodegeneration may have a closer relationship with symptom progression in MCI (Jack et al., 2008b) and mild to moderate AD dementia patients (Jack et al., 2009, 2008a; Hyman et al., 1991). Previous studies have shown that neurodegenerative processes are facilitated by

amyloid deposition (Pooler et al., 2015; Butterfield, 2002; Calhoun et al., 1998), suggesting that A β and neurodegeneration may interact at some point along the disease continuum. Overall, A β and neurodegeneration do not seem to provide entirely overlapping diagnostic information (Jack et al., 2008a).

Neurodegeneration in mild AD dementia has most consistently been found in medial and lateral temporo-parietal regions (Desikan et al., 2009; Jack et al., 2008a; Jack et al., 2009; Jack et al., 1997). Terms such as the 'signature' regions of AD, or constructs such as "STAND" (SStructural Abnormality INdex) (Dickerson et al., 2009; Vemuri et al., 2009), have been used to describe these AD-vulnerable clusters, and thickness in such aggregates have been found to predict cognitive

* Corresponding author at: Athinoula A. Martinos Center for Biomedical Imaging, 149 13th Street, Charlestown, MA 02129, USA.
E-mail address: patrizia@nmr.mgh.harvard.edu (P. Vannini).

<http://dx.doi.org/10.1016/j.nicl.2017.10.034>

Received 25 May 2017; Received in revised form 9 September 2017; Accepted 28 October 2017

Available online 31 October 2017

2213-1582/ © 2017 The Authors. Published by Elsevier Inc. This is an open access article under the CC BY-NC-ND license (<http://creativecommons.org/licenses/by-nc-nd/4.0/>).

decline or disease progression (Pettigrew et al., 2016; Eskildsen et al., 2013; Desikan et al., 2009; Dickerson et al., 2009; Querbes et al., 2009; Vemuri et al., 2009). Clinical decline has also been investigated using regional structural measures. For example, a previous study showed that greater rates of impairment in instrumental activities of daily living in MCI and mild AD dementia were associated with decreased cortical thickness in the inferior temporal cortex and supramarginal gyrus, and with lower levels of cerebrospinal fluid (CSF) A β (Marshall et al., 2014).

While widespread relationships between baseline cortical thickness and change in Clinical Dementia Rating Sum-of-Boxes (CDR-SB, Morris, 1997) – used to quantify clinical impairment – have been observed in MCI patients, CSF measures of A β -42 have not been shown to predict a change in CDR-SB (Fjell et al., 2010; Walhovd et al., 2010). However, in those studies, interactions between amyloid pathology and regional neurodegeneration were not examined (Marshall et al., 2014; Fjell et al., 2010; Walhovd et al., 2010) despite there being discordant relationships between amyloid and regional neurodegeneration in patients with AD dementia (Fjell et al., 2010; Jack et al., 2008a).

Two crucial questions remain unanswered: first, whether amyloid and neurodegeneration have interactive or independent associations with clinical decline across the AD spectrum, and second, whether these associations show different regional patterns in areas known to be susceptible to pathology. To that end, we investigated whether cortical thickness and amyloid deposition, as measured with Pittsburgh Compound B positron emission tomography (PiB-PET), have an interactive or independent effect on longitudinally-measured CDR-SB scores in MCI and mild AD individuals. We examined these associations in specific amyloid-vulnerable regions as determined from a whole-brain correlational approach. As amyloid is considered to potentiate neurodegeneration, we hypothesized that this approach would provide us with a set of regions to further investigate independent versus interactive effects without biasing toward regions that may have no association with A β . Additionally, to assess specificity of these findings, we also included the precentral motor cortex as a control region. Overall, having a better understanding of regional associations between A β , neurodegeneration, and clinical decline, contributes to the development of more sensitive measures for the diagnosis and prognosis of AD dementia.

2. Methods

2.1. Participants and behavioral measures

Forty-seven older adults [34% female, mean age = 72.52(8.29)] from an ongoing study on aging and AD dementia were included in the current study [Table 1]. Written informed consent was obtained prior to experimental procedures, and the study was approved and conducted, in accordance with the Partners Human Research Committee at the Massachusetts General Hospital and Brigham and Women's Hospital (Boston, MA).

All participants completed the Mini-Mental State Examination (MMSE, Folstein et al., 1975), the Clinical Dementia Rating scale (CDR, Morris, 1997), and an extensive neuropsychological test battery. Additionally, to assess clinical diagnosis at baseline, three experienced clinicians held a consensus meeting to review CDR and neuropsychological testing, a procedure explained in further detail in a previous study (Huijbers et al., 2015). Clinicians were blinded to the neuroimaging data during clinical assessment. The Clinical Dementia Rating Sum-of-Boxes (CDR-SB) [range: 0–18] was used to quantify clinical impairment, with higher scores indicating greater clinical decline. Forty-one participants received a diagnosis of amnesic MCI, single or multiple domain (Petersen, 2004), and six participants were diagnosed with AD dementia with amnesic symptoms (McKhann et al., 2011). All six mild AD dementia individuals, and 53.6% of MCI individuals, were A β +. Seven individuals (A β -: 1, A β +: 6) with diagnoses at follow-up were classified as having progressed in clinical diagnosis from MCI to

AD dementia, while twenty-six (A β -: 15, A β +: 11) remained 'stable' in their MCI diagnosis. Test metrics were acquired across 36 months from baseline [baseline (N = 47), 3 months (N = 31), 6 months (N = 33), 12 months (N = 34), 18 months (N = 27), 24 months (N = 21), and 36 months (N = 21)].

2.2. MRI acquisition

All participants underwent an anatomical magnetic resonance imaging (MRI) scan at baseline, on average 35.74 (SD = 34.85) days [median = 29, interquartile range (IQR) = 10.50, 51.50, minimum = 0, maximum = 197.0, days] from the baseline clinical visit – there were no significant differences between A β status (A β - or A β +) groups on these time differences [$t(45) = -0.68, p = 0.500$]. Data were acquired at the Athinoula A. Martinos Center for Biomedical Imaging using a Siemens Trio 3T system with a 12-channel phased array head coil. Foam pads were used to restrict head motion. The anatomical MRI consisted of a T₁-weighted magnetization-prepared rapid gradient-echo scan (MPRAGE, 256 sagittal slices, isotropic 1 mm, repetition time (TR) = 2300 ms, echo time (TE) = 2.98 ms, inversion time = 900 ms, flip angle = 9°, FOV = 270 × 253mm, matrix = 256 × 240, voxel size = 1.05 × 1.05 × 1.2 mm). Anatomical MRI data were analyzed using the standard processing pipeline within FreeSurfer v5.1. Technical details of the pipeline have been described in prior publications (Dale et al., 1999; Fischl and Dale, 2000; Fischl et al., 1999). White and pial surface segmentation was examined visually for quality assessment and edited when necessary. Cortical thickness values were mapped onto a semi-inflated surface of each participant's reconstructed brain. Maps were smoothed using a circularly symmetric Gaussian kernel of 15 mm full-width at half-maximum (FWHM), and averaged across participants using a non-rigid high-dimensional spherical averaging method aligning cortical folds. In accordance with the Desikan-Killiany atlas (Desikan et al., 2006), we separated a large cluster that encompassed the lateral, ventral, and medial aspects of the right hemisphere into two clusters, such that one cluster became a Lateral Temporo-Parietal cluster, and the second a Medial Temporal Lobe/Fusiform Gyrus cluster. Additionally, we separated a cluster that encompassed a large portion of the postero-medial and caudal dorsal aspect of the right hemisphere into a Precuneus cluster, a Lingual/Occipital cluster, and a Superior Parietal cluster [Fig. S1].

2.3. Amyloid PET imaging

Positron Emission Tomography (PET) imaging data were acquired on average 165.04 (SD = 203.43) days [median = 57.0, IQR = 25.0, 106.50, minimum = 0, maximum = 778.0, days] from the MRI measure – with no significant differences between A β groups [$t(45) = -0.34, p = 0.736$], and on average 165.04 (SD = 203.43) days [median = 88.0, IQR = 55.50, 137.50, minimum = 0, maximum = 812.0, days] from the baseline clinical visit – with no significant differences between A β status groups [$t(45) = -0.74, p = 0.461$]. Deposition of A β was measured using Pittsburgh Compound-B (PiB) [*N*-methyl-¹¹C]-2(4-methylaminophenyl)-6-hydroxy-benzothiazole] according to previously described methods (Johnson et al., 2007). In short: 60 min of dynamic PET data were acquired, following intravenous administration of [¹¹C] PiB, using an HR+ PET camera (Siemens) operating in 3D mode (image planes = 63, axial field of view = 15.2-cm, transaxial resolution = 5.6 mm, slice interval = 2.4 mm, 69 frames: 12 frames × 15 s, 57 frames × 60s). PET data were reconstructed and attenuation-corrected using standard Siemens software. Each frame was evaluated for head motion and adequate count statistics. Using Logan's graphical analysis method (Logan, 2000), we calculated PiB retention expressed as a distribution volume ratio (DVR) using a gray matter cerebellum reference region (Price et al., 2005).

Neocortical A β deposition was quantified using an aggregate DVR

Table 1
Sample demographics and characteristics.

	Entire sample (N = 47)	Aβ− (N = 19)	Aβ+ (N = 28)	Aβ− vs Aβ+ t or χ^2 scores, p-values
Age (years)	72.52 (8.29)	72.11 (9.39)	72.80 (7.61)	$t = -0.28, p = 0.780$
Education (years)	16.51 (2.69)	16.11 (2.87)	16.79 (2.57)	$t = -0.85, p = 0.400$
Sex (female %)	34	36	33	$\chi^2 = 0.01, p = 0.919$
MMSE	26.85 (2.29)	27.95 (1.39)	26.07 (2.50)	$t = 3.25, p = 0.002$
CDR global (0.5/1)	44/3	19/0	25/3	$\chi^2 = 2.18, p = 0.140$
CDR-SB	2.02 (1.33)	1.26 (0.63)	2.54 (1.44)	$t = -4.13, p = 0.0002$
MCI/AD dementia diagnosis	41/6	19/0	22/6	$\chi^2 = 4.67, p = 0.031$
β-amyloid (PiB DVR FLR)	1.41 (0.31)	1.09 (0.05)	1.63 (0.19)	$t = -14.37, p < 0.00001$
Global mean cortical thickness (mm)	2.35 (0.10)	2.40 (0.08)	2.32 (0.09)	$t = 3.11, p = 0.003$
N at 3 months follow-up	31	14	17	–
N at 6 months follow-up	33	15	18	–
N at 12 months follow-up	34	16	18	–
N at 18 months follow-up	27	14	13	–
N at 24 months follow-up	21	12	9	–
N at 36 months follow-up	21	12	9	–
Individuals that progressed to AD dementia status	6	0	6	–
Individuals that remained as MCI	26	15	11	–
Individuals with no follow-up diagnosis*	11	3 MCI	6 MCI, 2 AD	–

Values are means (standard deviation) or frequencies. AMNART VIQ, American National Adult Reading Test verbal intelligence quotient; MMSE, Mini-Mental State Examination; CDR-SB, Clinical Dementia Rating scale sum of boxes; MCI, mild cognitive impairment; AD, Alzheimer's disease dementia; Aβ, β-amyloid; PiB, Pittsburgh Compound-B (PiB) retention expressed as a distribution volume ratio (DVR) in neocortical regions of interest comprised of frontal, lateral temporal and retrosplenial (FLR) cortex. *Reasons for no follow-up diagnosis include having only one baseline time-point and no further follow-up visits, or unavailable diagnosis status at the follow-up visit used for our analyses.

from a set of regions that comprise association cortices, including the frontal, lateral parietal, lateral temporal, and retrosplenial cortices (FLR) (Klunk et al., 2004). A cut-off of PiB DVR > 1.2 indicated 'Aβ+' status classification (N = 28). This threshold was determined by a Gaussian mixture modeling approach (Mormino et al., 2014b) on an independent data sample with an identical amyloid PiB-PET protocol (Johnson et al., 2007). To note, we used a dichotomous PiB-PET measure rather than a continuous one in order to enhance the interpretability of the three-way interaction models; having a dichotomous measure allowed for an easier breakdown of the three-way interactions for visualization purposes.

2.4. Statistical analyses

All statistical analyses were performed in SPSS (IBM SPSS, version 21; IBM Corp., Armonk, NY, USA) and R software (R, version 3.2.2; R Foundation for Statistical Computing, Vienna, Austria). Group differences on demographics and neuropsychological measures at baseline were compared using one-sample and independent two-sample t-tests for continuous variables, and chi-square tests for comparing proportions.

To determine regions susceptible to amyloid pathology, we associated baseline cortical thickness with amyloid deposition within FreeSurfer v5.1. Surface maps of cortical thickness effects were generated regressing [C¹¹] PiB uptake in the FLR regions as a continuous predictor on every vertex of the surface, such that PiB was the predictor variable, and cortical thickness the dependent variable. Age was included as a covariate in the regression model.

Results were non-parametrically corrected for multiple comparisons by first performing a simulation to get a measure of the distribution of the maximum cluster size under the null hypothesis (α = 0.05) repeated over 1000 iterations. Data was then thresholded using the same level and sign, revealing clusters in a thresholded map (Hagler et al., 2006). For each cluster, p = probability of seeing a maximum cluster that size or larger during simulation. Mean cortical thickness values were then extracted from each cluster and used for off-line statistical analyses.

To first test whether baseline cortical thickness was associated with baseline CDR-SB, we used the extracted mean baseline cortical

thickness values from the amyloid-associated regions in linear regression models, using baseline CDR-SB as the dependent variable and cortical thickness as the independent variable. A separate regression analysis was performed for each cluster. All off-line models included age as a covariate [Table 2]. Results were Bonferroni-corrected (α = 0.05, p-threshold = 0.0056, 9 models considered).

Next, to attain estimates of progression of clinical decline over time, we performed linear mixed effects models (LMEs) using mean cortical thickness, Aβ status (Aβ− or Aβ+), and their interaction with time, to predict change in CDR-SB (over 167 observations). We conducted three models [Table 3]: the first model included only Aβ status (dichotomous), and its interaction with time; the second model included Aβ status, cortical thickness, and their interaction with time to probe for independent effects (the effects of cortical thickness from each significant cluster were assessed separately in different models); the third model included the three-way interaction of Aβ status × cortical thickness × time to investigate possible regional interactive effects on

Table 2
Baseline cortical thickness associations with baseline clinical impairment.

	CDR-SB (N = 47)	
	Estimate	p-Value
I. Model with only r.LTP thickness	− 3.13 (1.05)	0.0047**
II. Model with only r.MTL/FFG thickness	− 3.42 (0.83)	0.0002**
III. Model with only r.Precuneus thickness	− 3.34 (1.14)	0.0053**
IV. Model with only r.SP thickness	− 3.26 (1.12)	0.0055**
V. Model with only r.Caudal middle frontal thickness	− 4.25 (1.19)	0.0009**
VI. Model with only r.Lingual/occipital thickness	− 6.07 (1.15)	< 0.0001**
VII. Model with only l.Lateral occipital thickness	− 4.33 (1.26)	0.0014**
VIII. Model with only l.Precuneus thickness	− 5.24 (1.22)	< 0.0001**
IX. Model with only bh.Motor cortex thickness	− 2.80 (1.35)	0.0444

All models included age as a covariate, predicting CDR-SB. Results are listed as β estimate, then Standard Error of the Mean (SEM). Age and cortical thickness measures were continuous variables. Age, as a control variable, was centered at the group mean (72.55). CDR-SB, Clinical Dementia Rating Sum-of-Boxes; LTP, lateral temporo-parietal; MTL, medial temporal lobe; FFG, fusiform gyrus; SP, superior parietal; r, right; l, left. **p-value significant at Bonferroni-corrected level p < 0.0056 (α = 0.05, 9 models).

Table 3
Longitudinal models for cortical thickness and amyloid predicting CDR-SB change over time.

Model	Included variables	r.LTP	r.MTL/FFG	r.Precuneus	r.SP	r.CMF	r.Lingual/ occipital	l.Lateral occipital	l.Precuneus	bh.Motor	
I.	Only CTh × Time	β	−0.261	−0.081	−0.219	−0.168	−0.264	−0.240	−0.307	−0.255	−0.095
		SEM	(0.04)	(0.03)	(0.04)	(0.04)	(0.05)	(0.04)	(0.04)	(0.04)	(0.06)
		p	< 0.0001**	0.0038	< 0.0001**	< 0.0001**	< 0.0001**	< 0.0001**	< 0.0001**	< 0.0001**	0.0956
II.	Aβ × Time	β	0.024	0.052	0.030	0.042	0.032	0.030	0.029	0.022	0.055
		SEM	(0.01)	(0.01)	(0.01)	(0.01)	(0.01)	(0.01)	(0.01)	(0.01)	(0.01)
		p	0.0497	< 0.0001**	0.0150	0.0006**	0.0155	0.0266	0.0047	0.0667	< 0.0001**
	CTh × Time	β	−0.202	−0.011	−0.150	−0.083	−0.166	−0.157	−0.249	−0.198	−0.040
		SEM	(0.05)	(0.03)	(0.04)	(0.04)	(0.06)	(0.05)	(0.04)	(0.05)	(0.05)
		p	< 0.0001**	0.7154	0.0008**	0.0520	0.0058	0.0046	< 0.0001**	< 0.0001**	0.4508
III.	Aβ × Time	β	0.950	0.264	0.809	0.932	1.334	0.234	1.00	0.628	0.016
		SEM	(0.21)	(0.17)	(0.18)	(0.16)	(0.28)	(0.24)	(0.17)	(0.19)	(0.24)
		p	< 0.0001**	0.1203	< 0.0001**	< 0.0001**	< 0.0001**	0.3288	< 0.0001**	0.0015**	0.9464
	CTh × Time	β	−0.001	0.024	0.031	0.048	0.039	−0.071	−0.034	−0.030	−0.046
		SEM	(0.06)	(0.04)	(0.06)	(0.05)	(0.07)	(0.11)	(0.05)	(0.07)	(0.07)
		p	0.9856	0.5629	0.6087	0.2903	0.5871	0.5335	0.5182	0.6752	0.5409
	Aβ × CTh × Time	β	−0.358	−0.077	−0.343	−0.418	−0.520	−0.111	−0.440	−0.286	0.015
		SEM	(0.08)	(0.06)	(0.08)	(0.07)	(0.11)	(0.13)	(0.07)	(0.09)	(0.10)
		p	< 0.0001**	0.2104	< 0.0001**	< 0.0001**	< 0.0001**	0.3920	< 0.0001**	0.0021	0.8799

All LME models included age and its interaction with time as covariates, predicting CDR-SB (167 observations). Results are listed as β estimate, then Standard Error of the Mean (SEM), and lastly the corresponding p-value. Aβ Status was a dichotomous variable, and age and cortical thickness measures were continuous. Age, as a control variable, was centered at the group mean (73.89). CTh, cortical thickness; Aβ, β-amyloid; LME, linear mixed-effects model; CDR-SB, Clinical Dementia Rating Sum-of-Boxes; LTP, lateral temporo-parietal; MTL, medial temporal lobe; FFG, fusiform gyrus; SP, superior parietal; CMF, caudal middle frontal; bh, bilateral hemisphere; r, right; l, left. **p-value in Bold represents significance at Bonferroni-corrected level $p < 0.0019$ ($\alpha = 0.05$, 27 models).

CDR-SB change. All LMEs included age and its interaction with time as covariates, and included a random intercept for each participant. Results were Bonferroni-corrected ($\alpha = 0.05$, p-threshold = 0.0019, 27 models considered).

The fit of complex models was compared using the corrected-Akaike Information Criterion (AICc), a correction of the Akaike Information Criterion with a greater penalty for extra parameters in small data sets (decreasing the probability of selecting models that have many parameters). We also utilized the likelihood ratio and p-values from analyses of variance (ANOVAs) to assess the significance of the model comparisons [Table S1].

Lastly, to assess whether either a model with only Aβ burden or only medial temporal cortical thickness is better in predicting CDR-SB scores over time, we compared the Akaike weights of each LME model against the other. Specifically, we compared Akaike weights between Model I and Model III, and calculated an evidence ratio (Burnham et al., 2011).

To investigate whether our findings were restricted to brain regions demonstrating an association with Aβ burden (as defined by the vertex-wise analysis) or also seen in brain regions that show no association with Aβ burden, we also extracted cortical thickness values from a control region in the pre-central motor cortex as defined by the Desikan-Killiany atlas (Desikan et al., 2006) [Table 3].

To ensure that our effects were not driven by the inclusion of mild AD dementia cases, we performed additional LME models relating ROI cortical thickness to CDR-SB change in the MCI individuals only [Table S2].

Additionally, we performed a supplementary analysis investigating the contribution of intracranial volume corrected-hippocampal volume (HPV) on the three-way interactions found in Table 3 of ROI cortical thickness vs amyloid burden on CDR-SB change [Table S3]. This could help explain whether Aβ-neurodegeneration interactions predict clinical decline above HPV or not.

3. Results

3.1. Demographic characteristics by amyloid-status group

There were no significant differences between Aβ− and Aβ+ groups on any demographic variable [Table 1]. However, at baseline, Aβ+ individuals had lower MMSE scores ($p = 0.002$), and higher CDR-

SB scores (Fig. 2a, $p = 0.0002$), than Aβ− individuals.

3.2. The association between amyloid burden and whole-brain cortical thickness

Regressing Aβ deposition as a continuous variable on cortical thickness vertex-wise across the entire cortical surface revealed significant negative associations in clusters encompassing the right lateral temporo-parietal (LTP), right medial temporal lobe/fusiform gyrus (MTL/FFG), bilateral precuneus, right superior parietal (SP), right caudal middle frontal, right lingual/occipital, and left lateral occipital cortices ($p < 0.05$, cluster-wise corrected). Overall, at baseline, greater Aβ deposition was related with lower cortical thickness in an AD-like regional pattern [Fig. 1].

3.3. Aβ-associated baseline cortical thickness predicts baseline CDR-SB

Extracted baseline cortical thickness values from the right LTP, right MTL/FFG, right SP, right caudal middle frontal, right lingual/occipital, left lateral occipital, and bilateral precuneus, were associated with baseline CDR-SB scores (controlling for age, $p < 0.01$) [Table 2]. In contrast, baseline cortical thickness values from the bilateral motor cortex region did not show an association with baseline CDR-SB scores. Results are reported as significant after Bonferroni-correction ($\alpha = 0.05$, p-threshold = 0.0056, 9 models considered).

3.4. Increased Aβ burden predicts change in CDR-SB

After accounting for age and its interaction with time, we found that baseline categorical Aβ (Aβ− vs Aβ+) predicted CDR-SB change across time ($p < 0.0001$), such that CDR-SB increased more so for Aβ+ individuals, than Aβ− individuals [Fig. 2B].

3.5. Independent versus interactive effects of cortical thickness and Aβ burden on predicting CDR-SB change

Accounting for age and its interaction with time, we investigated whether cortical thickness and Aβ burden independently contributed to or interacted in predicting change in CDR-SB over time. We found that Aβ burden and cortical thickness from the right LTP [Fig. 3A], right

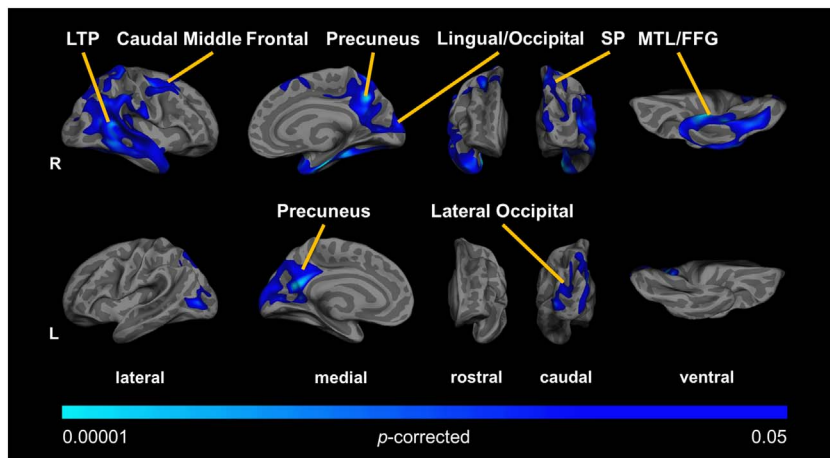


Fig. 1. Amyloid deposition is associated with cortical thickness across the cortical mantle. FLR (frontal, lateral temporal and retrosplenial) PiB (Pittsburgh Compound-B) retention was negatively associated with cortical thickness in the right lateral temporo-parietal (LTP), right medial temporal lobe/fusiform gyrus (MTL/FFG), bilateral precuneus, right superior parietal (SP), right caudal middle frontal, right lingual/occipital regions, and left lateral occipital cortex. Age, as a control variable, was centered at the group mean (73.89). Non-parametrically corrected for multiple comparisons at $p < 0.05$.

precuneus [Fig. 3B], right SP [Fig. 3C], right caudal middle frontal [Fig. 3D], and left lateral occipital clusters [Fig. 3E], interacted in predicting CDR-SB change over time [see Table 3], showing that cortical thickness in these clusters predicted CDR-SB longitudinally in $A\beta^+$ individuals, but not in $A\beta^-$ individuals.

For the right MTL/FFG cluster, the explained variance of baseline cortical thickness was completely shared with amyloid deposition, with amyloid being the strongest predictor of CDR-SB change [Table 3]. Left precuneus thickness explained significantly more variance than amyloid deposition in predicting CDR-SB change over time, and right lingual/occipital thickness predicted change over time, but without $A\beta$ in the model [Table 3].

Model fit comparisons between two-way (Thickness \times Time) and three-way interaction models ($A\beta$ Status \times Thickness \times Time) indicated that modeling the three-way interactions statistically predicted CDR-SB change better than assessing the independent effects of the two-way interactions (right LTP, bilateral precuneus, right superior parietal, right caudal middle frontal, and left lateral lingual/occipital, $p < 0.0001$; right MTL/FFG, right lingual/occipital, $p > 0.4$) [Table S1].

In terms of whether $A\beta$ burden predicted CDR-SB change better than medial temporal cortical thickness, we found that when comparing the AIC weights of a model with only $A\beta$ in it (AIC-weight = 0.9998) with a model with only MTL/FFG cluster thickness (AIC-weight = 0.0002), the $A\beta$ only model showed 4346.39 times more evidence (Burnham et al., 2011) of being the better model [see Fig. 4].

3.6. LME models using a control region

Lastly, in an LME model with precentral motor cortex thickness, covarying for age and its interaction with time, primary motor cortex thickness did not predict CDR-SB over time ($p = 0.0956$). Furthermore, in a model with both motor cortex thickness and $A\beta$ Status, covarying for age and its interaction with time, we found that while motor cortex thickness was not a significant predictor of CDR-SB over time ($p = 0.4508$), the effect of $A\beta$ Status \times Time was significant ($p < 0.0001$) [Table 3].

3.7. Supplementary analysis excluding mild AD cases

Additional post-hoc LME models relating ROI cortical thinning with CDR-SB change excluding all mild AD cases showed equal results as those found when including these individuals [Table S2].

3.8. Supplementary three-way interaction models, covarying for hippocampal volume

Additionally, while not part of the cortical mantle or our original analysis, we performed the original three-way interaction models while covarying for intracranial volume-corrected bilateral hippocampal volume (HPV), investigating the effect above and beyond hippocampal volume, and found that the results remained unchanged even with hippocampal volume in the models (i.e., results remained the same as in Table 3), [Table S3].

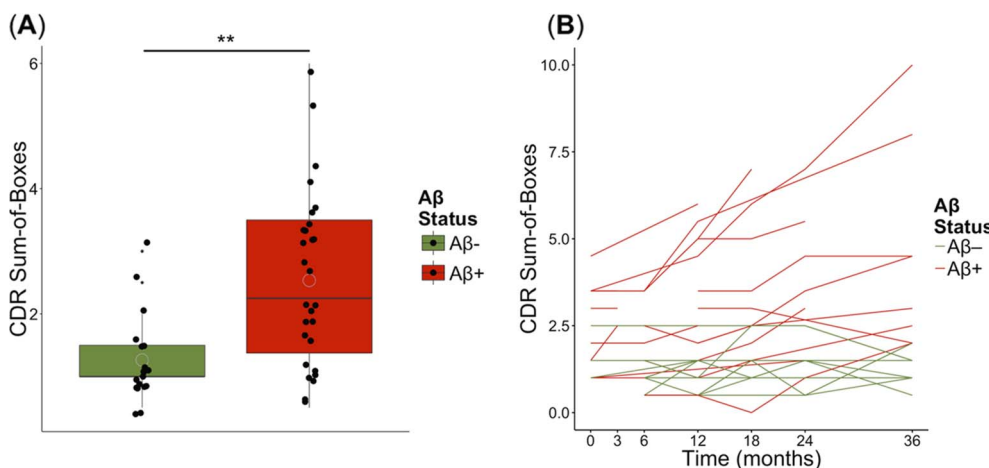


Fig. 2. CDR-SB by amyloid status. (A) At baseline, $A\beta^+$ individuals showed significantly greater CDR-SB (Clinical Dementia Rating Sum-of-Boxes) as compared to $A\beta^-$ individuals ($t = -4.13$, $SE = 0.31$, $**p = 0.0002$). (B) CDR-SB increase over time was observed across both groups ($\beta = 0.033$, $SE = 0.01$, $p < 0.0001$). While CDR-SB significantly increased in $A\beta^+$ individuals ($\beta = 0.068$, $SE = 0.01$, $p < 0.0001$), CDR-SB did not significantly increase in $A\beta^-$ individuals ($\beta = 0.005$, $SE = 0.004$, $p = 0.2434$). Model for (B) consisted of time, age centered at group mean (73.89), its interaction with time, and random individual intercepts.

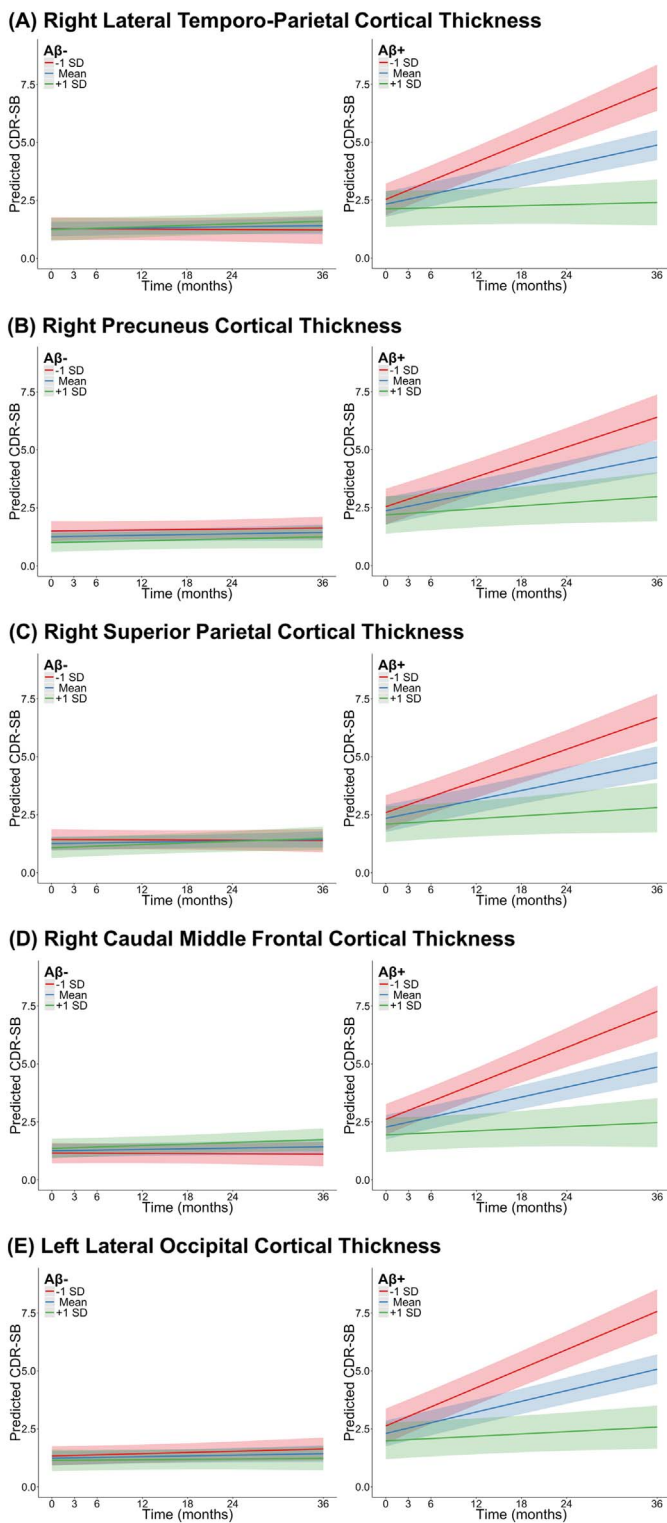


Fig. 3. Lower cortical thickness at baseline predicts CDR-SB increase over time depending on amyloid status.

Significant interactions of CDR-SB (Clinical Dementia Rating Sum-of-Boxes) over time by (A) right lateral temporo-parietal-thickness, (B) right precuneus-thickness, (C) right superior parietal-thickness, (D) right caudal middle frontal-thickness, (E) left lateral occipital-thickness. Colored lines represent: red, -1 standard deviation of the mean; blue, the mean; green, +1 standard deviation of the mean. Left Panel: Aβ- individuals; Right Panel: Aβ+ individuals. While lower cortical thickness in these regions at baseline predicted greater increase in CDR-SB over time in Aβ+ individuals ($p \leq 0.0001$, right column), lower cortical thickness in these regions at baseline in Aβ- individuals did not significantly predict change in CDR-SB ($p > 0.2$, left column). Models consisted of time, age centered at group mean (73.89), its interaction with time, and random individual intercepts.

4. Discussion

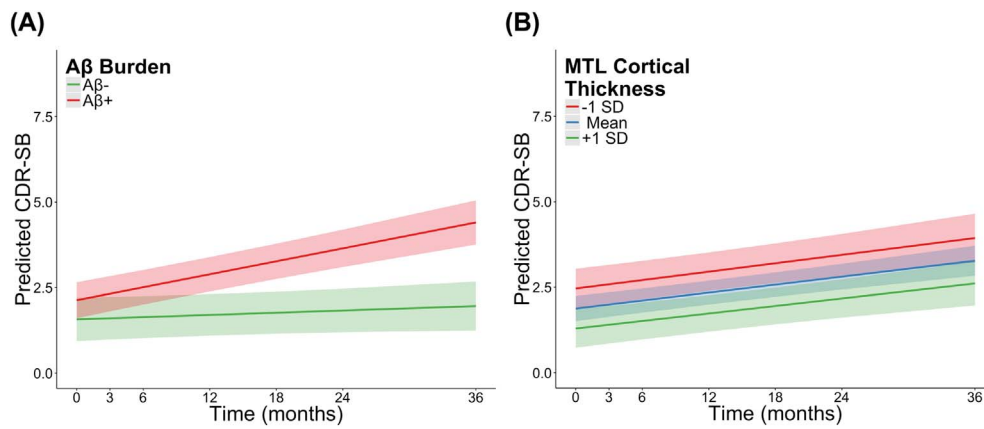
Here we aimed to investigate interactive and additive effects of amyloid and regional cortical thickness in predicting clinical decline over time. While previous studies have reported associations between CDR-SB increase and either cortical thickness in several regions or AD pathology, our study now shows that in memory impaired individuals, neocortical amyloid pathology and regional cortical thickness interact in predicting CDR-SB over time. Individuals with increased Aβ burden (Aβ+) and lower cortical thickness in right lateral temporo-parietal, right precuneus, right superior parietal, right caudal middle frontal, or left lateral occipital regions, showed greater CDR-SB over time than individuals with low Aβ burden (Aβ-). Interestingly, when considering medial temporal lobe (MTL) thickness, neocortical amyloid pathology explained much more variance to clinical decline than thickness. These findings support the notion that AD-related pathology found within the MTL could reflect various age-related changes (Price et al., 2009; Savva et al., 2009; Raz et al., 2004; Jernigan et al., 1991). For example, Braak Stage I/II/III occurs largely within the MTL but is not always characterized by cognitive deficits (Delacourte et al., 2002; Delacourte et al., 1999; Braak and Braak, 1991). Excluding mild AD individuals from our linear mixed-effects models revealed that all these relationships remained significant, further suggesting that lower cortical thickness values in specific regions, vulnerable to amyloid pathology, predict clinical decline already at the prodromal stage.

Previous studies in older cognitively normal individuals have found that high Aβ burden is associated with lower cortical thickness in a specific set of regions, consisting of lateral parietal and posterior cingulate regions extending into the precuneus (Doré et al., 2013; Dickerson and Wolk, 2012; Becker et al., 2011; Fortea et al., 2011; Dickerson et al., 2009). Here we demonstrate a similar topography using an exploratory whole-brain approach relating Aβ to cortical thickness, validating that these regions are susceptible to AD pathology.

Our results showing a relationship between baseline cortical thickness and baseline CDR-SB are in accordance with previous studies. For instance, Dickerson et al. (2009), showed that a combination of medial temporal, inferior temporal, and inferior frontal cortical thickness ROIs provides the best model for cross-sectionally predicting CDR-SB (Dickerson et al., 2009). Similarly, our findings of baseline cortical thickness predicting change in CDR-SB is consistent with the findings from Vemuri et al. (2009), who found that an abnormal global brain structure index (“STAND” method) at baseline predicted CDR-SB increase over time, and better than [CSF] Aβ alone, a relationship most prominent in AD dementia patients as compared with amnesic MCI or clinically normal individuals (Vemuri et al., 2009). Importantly however, while global markers can be valuable for predicting disease progression (Eskildsen et al., 2013) as they are easy to implement in clinical settings, regional information is lost when combining regions together, and this also adds noise to the prediction model.

In the current study, we found that cortical thickness of the right precuneus, right caudal middle frontal, left lateral occipital cortex, right superior parietal lobule and right lateral temporal cortex predicted clinical decline in Aβ+ individuals. In particular, we found that the Aβ+ group had more variability than the Aβ- group, driving these interactions (see Fig. 2a for a depiction of the variance between the two groups), such that Aβ- individuals declined slower than Aβ+ individuals. This validates previous findings and suggests that individuals with increased Aβ burden have increased regional neurodegeneration, which in turn predicts clinical decline, as compared to individuals with low Aβ burden. For example, the co-occurrence of high Aβ and neurodegeneration has been shown to be predictive of cognitive decline even in clinically-normal (CN) individuals (Mormino et al., 2014a). Our results are in accordance with these previous findings in CN, and extend into the prodromal and clinical stage of AD.

Our findings suggest, consistent with the amyloid-cascade hypothesis, that the predictive value for disease progression using neocortical



intercepts.

thickness values from amyloid-associated regions is stronger when cognitively impaired individuals are A β +, and these associations seem to be specific to regions vulnerable to amyloid pathology. For example, using a control region in the premotor cortex revealed no association with cortical thickness, nor an interaction between cortical thickness and amyloid burden on CDR-SB change. Although we acknowledge that caution should be made on the generalizability of these findings to other brain regions not detected in our vertex-wise analysis, these results suggest that the interaction of amyloid and cortical thickness presented in the manuscript is restricted to A β -associated cortical regions.

While MTL thickness (on its own) marginally predicted clinical decline, these associations were similar for A β + and A β - individuals, suggesting that the underlying structural correlates could be explained by a combination of both AD and non-AD pathology (see Freeze et al., 2017; Villeneuve et al., 2014). Jacobs et al. (2011) have previously shown that MTL atrophy alone is not sufficient in predicting conversion to AD dementia, and atrophy of the MTL has been previously related to normal aging (Raz et al., 2004; Jernigan et al., 1991). Furthermore, in CN individuals, MTL pathology may not necessarily be only related to amyloid (Mormino et al., 2016; Jagust and Mormino, 2011). This ultimately raises the question of whether thickness values across MTL regions behave differently, and whether they should potentially be excluded from future “signature” regions and aggregates for predicting clinical decline.

While we did not include hippocampal volume in our primary analyses as the hippocampus is not part of the cortical mantle and our approach was exploratory in that we used a voxel-wise surface-based approach, we conducted supplementary analyses investigating the influence of hippocampal volume on our longitudinal three-way interactions of cortical thickness \times A β status \times time, predicting CDR-SB change. Those results demonstrated that with hippocampal volume covaried for in the models, all relationships from our main analysis remained statistically significant, further supporting the possibility that atrophy in the MTL regions may not provide any additional information above A β burden and neocortical atrophy in relation to clinical decline.

While atrophy could be associated with several underlying pathologies, including vascular lesions, Lewy bodies, or neurofibrillary tangles, the spatial pattern of cortical thinning found in the current study seems, to some extent, spatially similar to the topography of tau pathology. Including information on tau pathology in models like the ones in the current study could further help elucidate the contribution of both A β and tau AD pathology markers on processes related to cortical thinning and clinical decline. For example, in preclinical AD patients, lower cortical thickness values in regions similar to the ones found in the current study have been shown to relate with higher levels of CSF phosphorylated tau (Pettigrew et al., 2016). Furthermore,

A β burden explains clinical decline better than medial temporal cortical thickness.

(A) A β Status significantly predicted CDR-SB (Clinical Dementia Rating Sum-of-Boxes) over time while controlling for medial temporal lobe (MTL) cortical thickness (A β Status \times Time: $\beta = 0.052$, SEM = 0.01, $p < 0.0001$). When removing A β Status \times Time from the model and running the models separately for A β groups, the effect was found to be driven by A β + individuals (MTL thickness \times Time: $\beta = -0.100$, SEM = 0.06, $p = 0.0834$) rather than A β - individuals (MTL thickness \times Time: $\beta = 0.022$, SEM = 0.03, $p = 0.4216$). (B) MTL cortical thickness, controlled for A β burden, did not predict CDR-SB over time ($\beta = -0.011$, SEM = 0.03, $p = 0.7154$). Models consisted of time, age centered at group mean (73.89), its interaction with time, and random individual

phosphorylated tau-dependent cortical thinning has been observed in amyloid positive individuals (Forste et al., 2014; Desikan et al., 2011), and A β -associated clinical decline has been shown to occur only in the presence of elevated phosphorylated tau (Pascoal et al., 2016; Desikan et al., 2012), demonstrating the complex, interacting relationships across molecular, morphological and clinical variables. To what extent tau pathology explains additional unique variance for predicting clinical decline within the context of amyloid pathology and cortical thinning can now be investigated with novel PET tau tracers (Johnson et al., 2016). For example, similarly to a previously found association between Flortaucipir (FTP) tau binding and temporo-parietal brain tissue loss in AD patients (Xia et al., 2017) and clinically normal individuals (LaPoint et al., 2017; Sepulcre et al., 2016), here we observe a similar spatial topography (e.g., in the temporo-parietal cortex) when relating A β to cortical thickness.

We acknowledge several limitations to our study. First, as we used baseline MRI and PET data, we cannot infer causality or direction of effect between A β retention and cortical thinning. Additionally, all individuals were highly educated, which could potentially provide cognitive reserve, delaying clinical decline in the context of brain pathology. Additionally, due to the relatively small sample size, future studies should reproduce the results found in the present study in larger samples. Furthermore, although there is no consensus regarding how to best capture clinical change, here we used the CDR as it includes a global and ‘sum-of-boxes’ score, combines a clinical interview and information from an informant, and has been shown to have excellent inter-rater reliability (Morris, 1997). In addition, the CDR-SB uses a continuous scale, which enhances its sensitivity for staging dementia severity across subjects as well as tracking individual changes over time (O’Byrne et al., 2008).

5. Conclusion

Using a surface-based whole-brain approach in a group of memory-impaired individuals, we found that greater neocortical A β was associated with lower cortical thickness consistent with previously reported structural patterns. Lower cortical thickness values predicted greater clinical decline over time in amyloid positive individuals, but not in amyloid negative individuals. However, associations between baseline medial temporal lobe thickness and clinical decline were similar for amyloid positive and amyloid negative individuals, and amyloid was overall a much stronger predictor of clinical decline than medial temporal lobe thickness. These relationships remained even when excluding patients with AD dementia. Overall, these findings may help reveal brain-behavior patterns that could enhance the prognosis of dementia among cognitively impaired individuals.

Disclosure statement

K.A. Johnson has provided consulting services for Lilly, Novartis, Janssen, Roche, Piramal, GE Healthcare, Siemens, ISIS Pharma, AZTherapy, and Biogen, received support from a joint NIH-Lilly-sponsored clinical trial (A4 Study U19AG10483), and received research support from NIH/National Institute on Aging (R01 AG046396, P01 AG036694, P50 AG00513421, U19AG10483, U01AG024904-S1), Fidelity Biosciences, the Michael J. Fox Foundation, and the Alzheimer's Association. R.A. Sperling reports serving as a paid consultant for AbbVie, Biogen, Bracket, Genentech, Lundbeck, Merck, Pfizer, Roche, and Sanofi; serving as a coinvestigator for Avid, Eli Lilly and Co, and Janssen Alzheimer Immunotherapy clinical trials; speaking at symposia sponsored by Eli Lilly and Co, Biogen, and Janssen; receiving research support from Janssen Pharmaceuticals and Eli Lilly and Co, relationships that are not related to the content in the manuscript; and receiving research support from the NIH, Fidelity Biosciences, Harvard NeuroDiscovery Center, and the Alzheimer's Association. F. d'Oleire Uquillas, H.I.L. Jacobs, B. Hanseeuw, G.A. Marshall, M. Properzi, A.P. Schultz, M.R LaPoint, and P. Vannini report no disclosures relevant to the manuscript.

Acknowledgements

This work was supported by the National Institutes of Health [K24 AG035007 and R01 AG027435 to R.A.S. and K.A.J., and K01AG048287 to P.V.]; the Alzheimer Nederland Fellowship [WE.15-2014-06 to H.I.L.J.], and the Alzheimer's Association [IIRG-06-27374 to R.A.S.]. This research was carried out in part at the Athinoula A. Martinos Center for Biomedical Imaging, using resources provided by the Center for Functional Neuroimaging Technologies [P41EB015896], a P41 Biotechnology Resource Grant supported by the National Institute of Biomedical Imaging and Bioengineering (NIBIB), National Institutes of Health. The content is solely the responsibility of the authors and does not necessarily represent the official views of the National Institute on Aging or the National Institutes of Health. We would also like to thank Olivia Hampton for her valuable input on the written manuscript.

Author contributions

R.A.S. and K.A.J. were responsible for the original experimental design. M.R.L., G.A.M., A.P.S., and M.P. collected the data and made the data available. M.R.L. and A.P.S. preprocessed the data. F.d.U., H.I.L.J., P.V., B.H., and R.A.S. performed data analysis and interpretation of findings. F.d.U., H.I.L.J., P.V., G.A.M., B.H., and R.A.S. wrote the manuscript, and all authors contributed to the final version.

Appendix A. Supplementary data

Supplementary data to this article can be found online at <https://doi.org/10.1016/j.nicl.2017.10.034>.

References

Becker, J.A., Hedden, T., Carmasin, J., Maye, J., Rentz, D.M., Putcha, D., ... Johnson, K.A., 2011. Amyloid-beta associated cortical thinning in clinically normal elderly. *Ann. Neurol.* 69 (6), 1032–1042.

Braak, H., Braak, E., 1991. Neuropathological staging of Alzheimer-related changes. *Acta Neuropathol.* 82, 239–259.

Burnham, K.P., Anderson, D.R., Huyvaert, K.P., 2011. AIC model selection and multi-model inference in behavioral ecology: some background, observations, and comparisons. *Behav. Ecol. Sociobiol.* 65, 23–35.

Butterfield, D.A., 2002. Amyloid beta-peptide (1-42)-induced oxidative stress and neurotoxicity: implications for neurodegeneration in Alzheimer's disease brain. A review. *Free Radic. Res.* 36 (12), 1307–1313.

Calhoun, M., Wiederhold, K.-H., Abramowski, D., Phinney, A.L., Sturchler-Pierrat, C., Staufenbiel, M., Sommer, B., Jucker, M., 1998. Neuron loss in APP transgenic mice. *Nature* 395, 755–756.

Dale, A.M., Fischl, B., Sereno, M.I., 1999. Cortical surface-based analysis. I. Segmentation

and surface reconstruction. *NeuroImage* 9 (2), 179–194.

Delacourte, A., David, J.P., Sergeant, N., Buée, L., Wattez, A., Vermersch, P., Ghazali, F., Fallet-Bianco, C., Pasquier, F., Lebert, F., Petit, H., Di Menza, C., 1999. The biochemical pathway of neurofibrillary degeneration in aging and Alzheimer's disease. *Neurology* 52, 1158–1165.

Delacourte, A., Sergeant, N., Wattez, A., Maurage, C.A., Lebert, F., Pasquier, F., David, J.P., 2002. Tau aggregation in the hippocampal formation: an aging or a pathological process? *Exp. Gerontol.* 37, 1291–1296.

Desikan, R.S., Segonne, F., Fischl, B., Quinn, B.T., Dickerson, B.C., Blacker, D., Buckner, R.L., Dale, A.M., Maguire, R.P., Hyman, B.T., Albert, M.S., Killiany, R.J., 2006. An automated labeling system for subdividing the human cerebral cortex on MRI scans into gyral based regions of interest. *NeuroImage* 31, 968–980.

Desikan, R.S., Cabral, H.J., Hess, C.P., et al., 2009. Automated MRI measures identify individuals with mild cognitive impairment and Alzheimer's disease. *Brain* 132, 2048–2057.

Desikan, R.S., McEvoy, L.K., Thompson, W.K., Holland, D., Roddey, J.C., Blennow, K., ... Alzheimer's Disease Neuroimaging, I., 2011. Amyloid-beta associated volume loss occurs only in the presence of phospho-tau. *Ann. Neurol.* 70 (4), 657–661.

Desikan, R.S., McEvoy, L.K., Thompson, W.K., Holland, D., Brewer, J.B., Aisen, P.S., ... Alzheimer's Disease Neuroimaging, I., 2012. Amyloid-beta-associated clinical decline occurs only in the presence of elevated P-tau. *Arch. Neurol.* 69 (6), 709–713.

Dickerson, B.C., Wolk, D.A., 2012. MRI cortical thickness biomarker predicts AD-like CSF and cognitive decline in normal adults. *Neurology* 78 (2), 84–90.

Dickerson, B.C., Bakkour, A., Salat, D.H., Feczko, E., Pacheco, J., Greve, D.N., ... Buckner, R.L., 2009. The cortical signature of Alzheimer's disease: regionally specific cortical thinning relates to symptom severity in very mild to mild AD dementia and is detectable in asymptomatic amyloid-positive individuals. *Cereb. Cortex* 19 (3), 497–510.

Doré, V., Villemagne, V.L., Bourgeat, P., Fripp, J., Acosta, O., Chetelat, G., et al., 2013. Cross-sectional and longitudinal analysis of the relationship between Abeta deposition, cortical thickness, and memory in cognitively unimpaired individuals and in Alzheimer disease. *JAMA Neurol.* 70, 903–911.

Eskildsen, S.F., Coupé, P., García-Lorenzo, D., Fonov, V., Pruessner, J.C., Collins, D.L., the Alzheimer's Disease Neuroimaging Initiative, 2013. Prediction of Alzheimer's disease in subjects with mild cognitive impairment from the ADNI cohort using patterns of cortical thinning. *NeuroImage* 65, 511–521.

Fischl, B., Dale, A.M., 2000. Measuring the thickness of the human cerebral cortex from magnetic resonance images. *Proc. Natl. Acad. Sci. U. S. A.* 97 (20), 11,050–11,055.

Fischl, B., Sereno, M.I., Dale, A.M., 1999. Cortical surface-based analysis. II: inflation, flattening, and a surface-based coordinate system. *NeuroImage* 9 (2), 195–207.

Fjell, A.M., Walhovd, K.B., Fennema-Notestine, C., McEvoy, L.K., Hagler, D.J., Holland, D., Brewer, J.B., Dale, A.M., Alzheimer's Disease Neuroimaging Initiative, 2010. CSF biomarkers in prediction of cerebral and clinical change in mild cognitive impairment and Alzheimer's disease. *J. Neurosci.* 30 (6), 2088–2101.

Folstein, M.F., Folstein, S.E., McHugh, P.R., 1975. "Mini-mental state". A practical method for grading the cognitive state of patients for the clinician. *J. Psychiatr. Res.* 12 (3), 189–198.

Fortea, J., Sala-Llonch, R., Bartres-Faz, D., Llado, A., Sole-Padullés, C., Bosch, B., et al., 2011. Cognitively preserved subjects with transitional cerebrospinal fluid beta-amyloid 1–42 values have thicker cortex in Alzheimer's disease vulnerable areas. *Biol. Psychiatry* 70, 183–190.

Fortea, J., Vilaplana, E., Alcolea, D., Carmona-Iragui, M., Sanchez-Saudinos, M.B., Sala, I., Anton-Aguirre, S., Gonzalez, S., Medrano, S., Pegueroles, J., Morenas, E., Clarimon, J., Blesa, R., Lleo, A., Alzheimer's Disease Neuroimaging Initiative, 2014. Cerebrospinal fluid B-amyloid and phospho-tau biomarker interactions affecting brain structure in preclinical Alzheimer disease. *Ann. Neurol.* 76 (2), 223–230.

Freeze, W.M., Jacobs, H.I., Gronenschild, E.H., Jansen, J.F., Burgmans, S., Aalten, P., Clerx, L., Vos, S.J., van Buchem, M.A., Barkhof, F., van der Flier, W.M., Verbeek, M.M., Rikkert, M.O., Backes, W.H., Verhey, F.R., the LeARN Project, 2017. White matter hyperintensities potentiate hippocampal volume reduction in non-demented older individuals with abnormal amyloid- β . *J. Alzheimers Dis.* 55 (1), 333–342.

Hagler, D.J., Saygin, A.P., Sereno, M.I., 2006. Smoothing and cluster thresholding for cortical surface-based group analysis of fMRI data. *NeuroImage* 33 (4), 1093–1103.

Huijbers, W., Mormino, E.C., Schultz, A.P., Wigman, S., Ward, A.M., Larvie, M., Amariglio, R.E., Marshall, G.A., Rentz, D.M., Johnson, K.A., Sperling, R.A., 2015. Amyloid- β deposition in mild cognitive impairment is associated with increased hippocampal activity, atrophy and clinical progression. *Brain* 138, 1023–1035.

Hyman, B.T., Flory, J.E., Arnold, S.E., et al., 1991. Quantitative assessment of ALZ-50 immunoreactivity in Alzheimer's disease. *J. Geriatr. Psychiatr. Neurol.* 4, 231–235.

Jack Jr., C.R., Petersen, R.C., Xu, Y.C., et al., 1997. Medial temporal atrophy on MRI in normal aging and very mild Alzheimer's disease. *Neurology* 49, 786–794.

Jack Jr., C.R., Lowe, V.J., Senjem, M.L., et al., 2008a. 11C PiB and structural MRI provide complementary information in imaging of Alzheimer's disease and amnesic mild cognitive impairment. *Brain* 131, 665–680.

Jack Jr., C.R., Weigand, S.D., Shiung, M.M., Przybelski, S.A., O'Brien, P.C., Gunter, J.L., Knopman, D.S., Boeve, B.F., Smith, G.E., Petersen, R.C., 2008b. Atrophy rates accelerate in amnesic mild cognitive impairment. *Neurology* 70, 1740–1752.

Jack Jr., C.R., Lowe, V.J., Weigand, S.D., et al., 2009. Serial PiB and MRI in normal, mild cognitive impairment and Alzheimer's disease: implications for sequence of pathological events in Alzheimer's disease. *Brain* 132, 1355–1365.

Jack Jr., C.R., Wiste, H.J., Lesnick, T.G., Weigand, S.D., Knopman, D.S., Vemuri, P., et al., 2013. Brain beta-amyloid load approaches a plateau. *Neurology* 80, 890–896.

Jacobs, H.I., van Bostel, M.P., van der Elst, W., Burgmans, S., Smeets, F., Gronenschild, E.H., Verhey, F.R., Uylings, H.B., Jolles, J., 2011. Increase the diagnostic accuracy of medial temporal lobe atrophy in Alzheimer's disease. *J. Alzheimers Dis.* 25 (3), 477–490.

- Jagust, W.J., Mormino, E.C., 2011. Lifespan brain activity, B-amyloid, and Alzheimer's disease. *Trends Cogn. Sci.* 15 (11), 520–526.
- Jernigan, T.L., Archibald, S.L., Berhow, M.T., Sowell, E.R., Foster, D.S., Hesselink, J.R., 1991. Cerebral structure on MRI, part 1: localization of age-related changes. *Biol. Psychiatry* 29, 55–67.
- Johnson, K.A., Gregas, M., Becker, J.A., Kinnecorn, C., Salat, D.H., Moran, E.K., ... Greenberg, S.M., 2007. Imaging of amyloid burden and distribution in cerebral amyloid angiopathy. *Ann. Neurol.* 62 (3), 229–234.
- Johnson, K.A., Schultz, A.P., Betensky, R.A., Becker, J.A., Sepulcre, J., Rentz, D., Mormino, E.C., Chhatwal, J., Amariglio, R.E., Papp, K., Marshall, G., Albers, M., Mauro, S., Pepin, L., Alverio, J., Judge, K., Philiossaint, M., Shoup, T., Yokell, D., Dickerson, B.C., Gomez-Isla, T., Hyman, B.T., Vasdev, N., Sperling, R.A., 2016. Tau positron emission tomographic imaging in aging and early Alzheimer disease. *Ann. Neurol.* 79 (7), 110–119.
- Klunk, W.E., Engler, H., Nordberg, A., Wang, Y., Blomqvist, G., Holt, D.P., ... Langstrom, B., 2004. Imaging brain amyloid in Alzheimer's disease with Pittsburgh Compound-B. *Ann. Neurol.* 55 (3), 306–319.
- LaPoint, M.R., Chhatwal, J.P., Sepulcre, J., Johnson, K.A., Sperling, R.A., Schultz, A.P., 2017. The association between tau PET and retrospective cortical thinning in clinically normal elderly. *NeuroImage* 157, 612–622.
- Logan, J., 2000. Graphical analysis of PET data applied to reversible and irreversible tracers. *Nucl. Med. Biol.* 27 (7), 661–670.
- Marshall, G.A., Lorus, N., Locascio, J.J., Hyman, B.T., Rentz, D.M., Johnson, K.A., Sperling, R.A., 2014. Regional cortical thinning and cerebrospinal biomarkers predict worsening daily functioning across the Alzheimer's disease spectrum. *J. Alzheimers Dis.* 41 (3), 719–728.
- McKhann, G.M., Knopman, D.S., Chertkow, H., Hyman, B.T., Jack, C.R., Kawas, C.H., Klunk, W.E., Koroshetz, W.J., Manly, J.J., Mayeux, R., Mohs, R.C., Morris, J.C., Rossor, M.N., Scheltens, P., Carrillo, M.C., Thies, B., Weintraub, S., Phelps, C.H., 2011. The diagnosis of dementia due to Alzheimer's disease: recommendations from the National Institute on Aging and the Alzheimer's Association workgroup. *Alzheimers Dement.* 7 (3), 263–269.
- Mormino, E.C., Betensky, R.A., Hedden, T., Schultz, A.P., Amariglio, R.E., Rentz, D.M., Johnson, K.A., Sperling, R.A., 2014a. Synergistic effect of B-amyloid and neurodegeneration on cognitive decline in clinically normal individuals. *JAMA Neurol.* 71 (11), 1379–1385.
- Mormino, E.C., Betensky, R.A., Hedden, T., Schultz, A.P., Ward, A., Huijbers, W., ... Harvard Aging Brain, S, 2014b. Amyloid and APOE e4 interact to influence short-term decline in preclinical Alzheimer disease. *Neurology* 82 (20), 1760–1767.
- Mormino, E.C., Papp, K.V., Rents, D.M., Schultz, A.P., LaPoint, M., Amariglio, R., Hanseeuw, B., Marshall, G.A., Hedden, T., Johnson, K.A., Sperling, R.A., 2016. Heterogeneity in suspected non-Alzheimer disease pathophysiology among clinically normal older individuals. *JAMA Neurol.* 73 (10), 1185–1191.
- Morris, J.C., 1997. Clinical dementia rating: a reliable and valid diagnostic and staging measure for dementia of the Alzheimer type. *Int. Psychogeriatr.* 9 (1), 173–178.
- O'Bryant, S.E., Waring, S.C., Munro Cullum, C., Hall, J., Lacritz, L., Massman, P.J., Lupo, P.J., Reisch, J.S., Doody, R., Texas Alzheimer's Research Consortium, 2008. Staging dementia using Clinical Dementia Rating Scale Sum of Boxes scores: a Texas Alzheimer's research consortium study. *Arch. Neurol.* 65 (8), 1091–1095.
- Pascoal, T.A., Mathotaarachchi, S., Shin, M., Benedet, A.L., Mohades, S., Wang, S., ... Alzheimer's disease Neuroimaging, I, 2016. Synergistic interaction between amyloid and tau predicts the progression to dementia. *Alzheimers Dement.* <http://dx.doi.org/10.1016/j.jalz.2016.11.005>.
- Petersen, R.C., 2004. Mild cognitive impairment as a diagnostic entity. *J. Intern. Med.* 256, 183–194.
- Pettigrew, C., Soldan, A., Zhu, Y., Wang, M.C., Moghekar, A., Brown, T., ... Team, B.R., 2016. Cortical thickness in relation to clinical symptom onset in preclinical AD. *NeuroImage Clin.* 12, 116–122.
- Pooler, A.M., Polydoro, M., Maury, E.A., Nicholls, S.B., Reddy, S.M., Wegmann, S., William, C., Saqrán, L., Cagsal-Getkin, O., Pitsstick, R., Beier, D.R., Carlson, G.A., Spiers-Jones, T.L., Hyman, B.T., 2015. Amyloid accelerates tau propagation and toxicity in a model of early Alzheimer's disease. *Acta Neuropathol. Commun.* 3, 14. <http://dx.doi.org/10.1186/s40478-015-0199-x>.
- Price, J.C., Klunk, W.E., Lopresti, B.J., Lu, X., Hoge, J.A., Ziolkó, S.K., ... Mathis, C.A., 2005. Kinetic modeling of amyloid binding in humans using PET imaging and Pittsburgh Compound-B. *J. Cereb. Blood Flow Metab.* 25 (11), 1528–1547.
- Price, J.L., McKeel, D.W., Buckles, V.D., Roe, C.M., Xiong, C., Grudman, M., Hansen, L.A., Petersen, R.C., Parisi, J.E., Dickson, D.W., Smith, C.D., Davis, D.G., Schmitt, F.A., Markesbery, W.R., Kaye, J., Krulan, R., Hulette, C., Kurland, B.F., Higdon, R., Kukull, W., Morris, J.C., 2009. Neuropathology of nondemented aging: presumptive evidence for preclinical Alzheimer's disease. *Neurobiol. Aging* 30 (7), 1026–1036.
- Querbes, O., Aubry, F., Pariente, J., Lotterie, J.A., Demonet, J.F., Duret, V., Puel, M., Berry, I., Fort, J.C., Celsis, P., the Alzheimer's Disease Neuroimaging Initiative, 2009. Early diagnosis of Alzheimer's disease using cortical thickness: impact of cognitive reserve. *Brain* 132, 2036–2047.
- Raz, N., Rodrigue, K.M., Head, D., Kennedy, K.M., Acker, J.D., 2004. Differential aging of the medial temporal lobe. *Neurology* 62, 433–438.
- Savva, G.M., Wharton, S.B., Ince, P.G., Forster, G., Matthews, F.E., Brayne, C., 2009. Age, neuropathology, and dementia. *N. Engl. J. Med.* <http://dx.doi.org/10.1056/NEJMoa0806142>.
- Selkoe, D.J., Hardy, J., 2016. The amyloid hypothesis of Alzheimer's disease at 25 years. *EMBO Mol. Med.* 8 (6), 595–608.
- Sepulcre, J., Schultz, A.P., Sabuncu, M., Gomez-Isla, T., Chhatwal, J., Becker, A., Sperling, R.A., Johnson, K.A., 2016. In vivo tau, amyloid, and gray matter profiles in the aging brain. *J. Neurosci.* 36 (28), 7364–7374.
- Sperling, R.A., Aisen, P.S., Beckett, L.A., Bennett, D.A., Craft, S., Fagan, A.M., et al., 2011. Toward defining the preclinical stages of Alzheimer's disease: recommendations from the National Institute on Aging-Alzheimer's Association workgroups on diagnostic guidelines for Alzheimer's disease. *Alzheimers Dement.* 7, 280–292.
- Vemuri, P., Wiste, H.J., Weigand, M.S., Shaw, L.M., Trojanowski, J.Q., Weiner, M.W., Knopman, D.S., Petersen, R.C., Jack Jr., C.R., on behalf of the Alzheimer's Disease Neuroimaging Initiative, 2009. MRI and CSF biomarkers in normal, MCI, and AD subjects: predicting future clinical change. *Neurology* 73 (4), 294–301.
- Villemagne, V.L., Pike, K.E., Chételat, G., Ellis, K.A., Mulligan, R.S., Bourgeat, P., Ackermann, U., Jones, G., Szoeke, C., Salvado, O., Martins, R., O'Keefe, G., Mathis, C.A., Klunk, W.E., Ames, D., Masters, C.L., Rowe, C.C., 2011. Longitudinal assessment of AB and cognition in aging and Alzheimer disease. *Ann. Neurol.* 69 (1), 181–192.
- Villemagne, V.L., Burnham, S., Bourgeat, P., Brown, B., Ellis, K.A., Salvado, O., et al., 2013. Amyloid beta deposition, neurodegeneration, and cognitive decline in sporadic Alzheimer's disease: a prospective cohort study. *Lancet Neurol.* 12, 357–367.
- Villeneuve, S., Reed, B.R., Wirth, M., Haase, C.M., Madison, C.M., Ayakta, N., ... Jagust, W.J., 2014. Cortical thickness mediates the effect of beta-amyloid on episodic memory. *Neurology* 82 (9), 761–767.
- Walhovd, K.B., Fjell, A.M., Brewer, J., McEvoy, L.K., Fennema-Notestine, C., Hagler, D.J., Jennings, R.G., Karow, D., Dale, A.M., Alzheimer's Disease Neuroimaging Initiative, 2010. Combining MR imaging, positron-emission tomography, and CSF biomarkers in the diagnosis and prognosis of Alzheimer's disease. *AJNR Am. J. Neuroradiol.* 31 (2), 347–354.
- Walsh, D.M., Teplow, D.B., 2012. Alzheimer's disease and the amyloid β -protein. *Prog. Mol. Biol. Transl. Sci.* 107, 101–124.
- Xia, C., Makarets, S.J., Caso, C., McGinnis, S., Gomperts, S.N., Sepulcre, J., Gomez-Isla, T., Hyman, B.T., Schultz, A.P., Vasdev, N., Johnson, K.A., Dickerson, B.C., 2017. Association of in vivo [18F]AV-1451 Tau PET imaging results with cortical atrophy and symptoms in typical and atypical Alzheimer's disease. *JAMA Neurol.* <http://dx.doi.org/10.1001/jamaneurol.2016.5755>.